SAND99-1946J

Kinetics and Mechanisms of Formation of Magnesite from Hydromagnesite in Brine

Peng-Chu Zhang*, Howard L. Anderson, Jr., John W. Kelly,
James L. Krumhansl, and Hans W. Papenguth
Sandia National Laboratories, Albuquerque, New Mexico, 87185-0750, USA

*corresponding author, Geochemistry Department, MS 0750, Sandia National Laboratories, Albuquerque, NM 87185 USA. Telephone: (505) 844-2669, email: pzhang@sandia.gov

DISCLAIMER

DISCLAIMER

Abstract

Reaction of brucite [$Mg(OH)_2$] with CO_2 produces various metastable hydrous magnesium carbonates, which will eventually mature to the only thermodynamically stable phase, magnesite ($MgCO_3$). Natural analog systems suggest that, at ambient temperatures, the transformation from a key metastable phase, hydromagnesite [$4MgCO_3 \bullet Mg(OH)_2 \bullet 4H_2O$], requires hundreds of years. A suite of experiments were conducted to elucidate mechanisms of transformation of hydromagnesite to magnesite by varying ionic strength and concentrations of magnesium and sulfate, and reacting hydromagnesite at temperatures between 110, 150 and 200°C. Arrhenius equations were used to extrapolate rate information collected at elevated temperature down to 25°C. An "induction" period, an interval of minimal transformation, was observed in all experiments. At 25°C, the induction period is estimated to require 18 to 200 years, with longer times attributed to higher magnesium concentrations. Once the induction period is completed, and more rapid transformation begins, the corresponding "half-lives" of hydromagnesite are about 4.7 and 73 years. Activation energies for the rapid transformation period were estimated to be between 81 and 100 kJ/mol. Transformation rates increased with increased ionic strength and decreased magnesium concentration. Sulfate concentration indirectly affected rates, by reducing magnesium activity through complexation. Two mechanisms for the transformation are supported. In brines with low magnesium concentration, hydromagnesite dehydration with concomitant formation of brucite and magnesite is favored. In brines with high magnesium concentration, a hydromagnesite dissolution – magnesite precipitation process is favored. Those mechanisms are also supported by Transmission Electron Microscopy (TEM) observations of reaction products.

Introduction

The Waste Isolation Pilot Plant (WIPP), a licensed repository for permanent disposal of defense-related transuranic nuclear waste, is situated in Permian bedded halite of the Salado Formation, in southeastern New Mexico, USA (US DOE, 1996). The inventory for the repository contains a

significant mass of organic-rich laboratory debris contaminated with traces of actinide elements, such as plutonium. An MgO backfill will be placed adjacent to the waste to scavenge carbon dioxide produced as the waste is degraded by microbial activity (Bynum et al., 1999). The primary purpose of the backfill is to control aqueous chemical conditions (pH and pCO_2) to minimize actinide solubilities, which will minimize predicted releases. Consequently, understanding the details of how this backfill will evolve chemically is of considerable importance. The nature of the magnesium carbonate mineral formed will affect chemical conditions controlling actinide solubilities. In addition, formation of hydrous mineral phases, including brucite [$Mg(OH)_2$] and hydrous magnesium carbonates, will impact the water budget of the repository. Among the minerals formed in the MgO-CO_2-H_2O systems, the anhydrous phase, magnesite ($MgCO_3$) is the only thermodynamically stable mineral at room temperature, or the WIPP-relevant temperature of 27°C (Langmuir, 1965; Lippmann, 1973). The kinetics of maturation of hydrous magnesium carbonate phases to magnesite affect the repository water saturation and chemical conditions, and must be considered in assessments of repository performance. The objective of the work described herein, therefore, is to develop an understanding of the kinetics of magnesite formation under WIPP-relevant conditions, to facilitate improved understanding of aqueous chemical conditions in the repository setting.

Thermodynamics and Kinetics of the MgO-CO_2-H_2O System

The general thermodynamic constraints on the MgO-CO_2-H_2O system are understood relatively well [Langmuir, 1965 #38; Lippmann, 1973 #40]. In the presence of liquid water, brucite is the thermodynamically stable solid, until the carbon dioxide partial pressure reaches a value of about $10^{-6.3}$ atm, above which anhydrous magnesium carbonate (magnesite) becomes stable (Lippmann, 1973, Figure 33). However, superimposed on this relationship are metastability fields for hydromagnesite [$4MgCO_3 \bullet Mg(OH)_2 \bullet 4H_2O$] and nesquehonite ($MgCO_3 \bullet 3H_2O$). At 25°C, the brucite-hydromagnesite boundary occurs at a carbon dioxide partial pressure of about $10^{-4.4}$ atm and the stability boundary between hydromagnesite and nesquehonite occurs when the partial pressure of carbon dioxide reaches a value of about 10^{-2} atm (Lippmann, 1973, Figure 33).

We expect that carbon dioxide generation in the WIPP will be quite slow, creating carbon dioxide partial pressures below the nesquehonite metastability field. Other experimental work in WIPP brines shows that hydromagnesite forms to the complete exclusion of magnesite (Papenguth et al., 1999). The thermodynamic relationships described above indicates this to be a transient situation, but provides no insight into the time needed for transformation of hydromagnesite to the stable magnesite phase. The kinetics of maturation are complex, in spite of the small number of chemical components in the MgO-CO_2-H_2O system. In this regard, the formation of magnesite has similarities to the difficulty geochemists have faced in understanding the formation of dolomite at ambient temperature (see, for example, Brady et al., 1996).

Some insight into the likely kinetics of this transition can be gained from examination of natural hydromagnesite occurrences. The most comprehensive description relates to occurrences in brackish ephemeral lakes associated with a lagoon complex in southeastern Australia (Alderman, 1965; von der Borch, 1965). In lakes, assemblages of hydromagnesite-aragonite and magnesite-dolomite (but not hydromagnesite-magnesite in the same sediment) are observed forming in recent marine sediments. Also, the assemblage aragonite-magnesite is observed within one foot of the surface in dried sediments from ancient Lake Bonneville, Utah (Graf et al., 1961). This stratum was dated at 11,300 (±250) years. Clearly, the transformation of hydromagnesite to magnesite may be rapid enough to be relevant in assessments of WIPP performance for the period of regulatory concern (10,000 years). In contrast, under other geochemical conditions, the transformation to magnesite may be quite slow. For example, Stamatakis (1995) described a commercial grade deposit of hydromagnesite and huntite plus lesser amounts of magnesite of upper Neogene age and suggests that hydromagnesite-aragonite assemblages occur in rocks as old as Tertiary age.

The transformation of hydromagnesite to magnesite is complicated by the fact that hydromagnesite contains an MgO component in addition to water and magnesium carbonate. The transformation may occur by (1) supplying additional CO_2 to complete the carbonation, or, (2) allowing sufficient time for the material to decompose into the thermodynamically favored mixture of magnesite, brucite and water. Sayles and Fyfe (1973) conducted an experimental

study at 126°C, supplying additional CO_2 and found that, occasionally, brucite was present as a reaction product. They used fluids with ionic strengths of 0.005 to 0.05 M. Despite the relatively low ionic strengths used, a number of their findings have qualitative bearing on the present work. First, elevated Mg levels were found to impede the transformation process. Second, increasing the ionic strength accelerated the reaction. Third, increasing the solid to fluid ratio increased the reaction rate. Fourth, a two-step reaction process was observed with an initial induction period during which no transformation was observed, and after which the rate accelerated with a fourth-order time dependence (t^4). Sayles and Fyfe (1973) attributed this latter observation to a variety of processes, relating both to the formation of initial magnesite nuclei and then to the slow growth of magnesite even in the presence of these nucleation centers. The time required for the solutions to achieve saturation, or the degree of super-saturation, seems not to be implicated in the delay.

Materials and Procedures

Materials

Reagent-grade hydromagnesite used in this study was obtained from Eastman Kodak Company (Rochester, New York). The material was examined using powder X-ray diffraction (XRD) and confirmed as a pure and well-crystallized hydromagnesite (Figure 1a). Natural magnesite, used for constructing the calibration curve, was obtained from Ward's Natural Science Establishment Inc. (Rochester, New York). The XRD spectrum for magnesite showed that no other minerals were present in detectable amounts (Figure 1b).

Two brines were used in the experiments: saturated NaCl solutions and a WIPP-specific brine simulant. The chemical composition of the WIPP-specific brine simulant is modeled after brines that may seep into the WIPP repository from the Salado Formation (Table 1). Its composition is based on comprehensive analyses of fluid samples collected from "weeps" within the WIPP repository (hence its name, generic weep, or "GW," brine; Krumhansl et al., 1991). Other brines

that may enter the WIPP repository more closely represent the pure NaCl solutions, also used in the experiments.

An additional set of experiments was conducted in brines in which the ionic strengths, $MgCl_2$ concentration, and $MgSO_4$ concentration were systematically varied, to assess the impact of the components found in the brines. Four sets of solutions were tested: (1) various concentrations of NaCl; (2) GW brine with various $MgCl_2$ concentrations; (3) saturated NaCl solutions with various amount of $MgCl_2$; and (4) saturated NaCl with various amounts $MgSO_4$.

Table 1. Chemical composition of GW brine

Reagent	Mass Fraction	
	g in 1.000 kg water	g in 1.000 L water
Na_2SO_4	20.684	25.234
NaBr	2.246	2.739
$Na_3B_4O_7 \cdot 10H_2O$	12.343	15.058
NaCl	147.22	179.61
KCl	28.553	34.835
$MgCl_2 \cdot 6H_2O$	169.71	207.05
LiCl	0.152	0.186
$CaCl_2 \cdot 2H_2O$	1.666	2.032
Deionized H_2O	617.43	753.26
Total mass	1000.00 g	1222.00 g
Total volume	819.67 mL	1000.00 mL

Procedures

XRD Calibration Curve

A hydromagnesite-magnesite calibration curve was constructed using integrated peak areas from powder XRD patterns collected with a Philips-Norelco instrument, using nickel-filtered Cu-Kα radiation and a diffracted-beam graphite monochromator. Analyses were conducted using a step size of 0.05° 2θ and a counting time of 4-seconds per step, equivalent to scanning rate of 0.75° 2θ/minute. Powders mounted on glass petrography slides were scanned from 10.00 to 45.00° 2θ,

a range that includes the 100 intensity hydromagnesite (011) and magnesite (104) peaks (Joint Committee on Powder Diffraction data cards 25-513 and 08-479, respectively). To minimize XRD analytical error, duplicate calibration analyses were made with magnesite contents of 0, 5, 10, 20, 25, 30, 40, 50, 75, 80, 90, 95, and 100 wt% by XRD. In this study, the peak ratio was calculated as:

$$R_{peak} = P_1/(P_1 + P_2) \quad (1)$$

where P_1 and P_2 are the integrated XRD peak areas for magnesite and hydromagnesite, respectively. R_{peak} is plotted against weight fraction magnesite in Figure 2. The minimum quantification limit of magnesite is about 3-5 wt%, which is similar to that reported by Sayles and Fyfe (1973).

Transformation Rate Experiments

At room temperature, the transformation rate of hydromagnesite to magnesite is too slow to be measured experimentally. Consequently, elevated temperatures of 110, 150 and 200°C (all ±4°C), were used to accelerate transformation. The Arrhenius equation was then used to estimate rates at room temperature.

Transformation experiments were conducted in small titanium autoclaves. A 0.30-g mass of hydromagnesite was placed in the autoclave along with 1.50 g of brine. Assembled autoclaves were placed in a pre-heated sand bath in an oven at the desired temperature. Periodic sampling and analysis allowed the extent of transformation to be monitored. Samples were collected on filter paper after quenching the autoclave in water. Samples were washed with deionized water to remove the soluble salts prior to preparation for XRD analysis. The time intervals of sampling were dependent upon the temperature and the type of brine used. Days to weeks were required for measurable transformation at 110 and 150°C, but at 200°C, significant transformation occurred in several hours. The additional set of four experiments were conducted at 200°C for

120 minutes, a combination selected that allowed complete transformation in the saturated NaCl solution.

Transmission Electron Microscopy

The samples for TEM studies were prepared by depositing annealed powder (reaction products) on holy-carbon-coated Cu-grids. All TEM and electron diffraction results were carried out with a JEOL 2010 HRTEM with an Oxford Link ISIS EDS system. The accelerating voltage of 200KeV was used. The point-to-point resolution of the HRTEM is 0.19 nm. Relatively low electron beam dose was used for the TEM imaging of hydromagnesite-bearing reaction products, in order to reduce electron beam damage of the hydromagnesite.

Results and Discussion

Transformation Rates

Figure 3 illustrates the changes in mineralogical composition during the hydromagnesite to magnesite transformation. The patterns in Figure 3 are typical in that no phases other than the original hydromagnesite and newly formed magnesite and brucite are evident. The absence of intermediate phases is consistent with trends observed in natural transformation processes [Spotl, 1994 #8] in which shrinkage (that is, dehydration) of hydromagnesite coincides with magnesite formation, without the presence of other phases. Since no external supply source of CO_2 was provided in our experiments, brucite would not be transformed into magnesite as described by Davies and Bubela (1973).

The transformation rates of hydromagnesite to magnesite in GW brine and saturated NaCl brine are summarized in Table 2 and they are also illustrated in Figure 4.

Table 2. Amount of hydromagnesite transformed to magnesite in two brines at three temperatures (expressed in weight percent*).

	Saturated NaCl			GW Brine		
Time (hour)	200°C	150°C	110°C	200°C	150°C	110°C
0.5	4.0					
1	5.4					
1.5	16					
2	91			1.8		
2.5	96			2.1		
3				3.9		
4				4.5		
5				24		
8		2.5		77		
10		3.5				
14		39				
17		52				
20		91				
48					1.9	
72					3.1	
96					4.5	
120					11	
144					18	
168					57	
216					77	
Time (day)						
9			2.0			
13			2.7			
14			2.8			
19			11			
22			42			
25			94			
38						4.5
53						6.6
65						14
74						23
92						55

*Note: XRD data were converted to wt% magnesite using the equation in Figure 2; the average standard analytical error was 1.11 wt%.

Transformation of hydromagnesite to magnesite in a saturated NaCl solution is substantially more rapid than that in the GW brine at all the three temperatures. In addition, there is clearly a profound effect of temperature. As demonstrated in Table 2 and Figure 4, the time required for complete transformation in the NaCl brine is similar to the time required to only initiate the reaction in GW brine.

Estimation of Transformation Rates at Room Temperature

The transformation of hydromagnesite to magnesite is assumed to be a first-order reaction. The equation used to calculate rate coefficients is the following, expressed in terms of the reactant, hydromagnesite:

$$\ln(M/M_0) = -kt \qquad (2)$$

where k (in $hours^{-1}$) is reaction rate coefficient, M/M_0 is the fraction of the hydromagnesite transformed at reaction time t (in hours), relative to the initial amount, M_0. By plotting the fraction transformed as a function of reaction time, the reaction rate coefficient is obtained by determining the slope of the relationship. In Table 3, the calculated reaction rate coefficients are compiled for the experiments described above.

Table 3. Measured reaction rate coefficients [k (in $hour^{-1}$)] for the transformation of hydromagnesite to magnesite (value in parentheses is the regression coefficient, R^2).

Brine	200°C	150°C	110°C
	k (R^2)		
GW brine	0.308 (0.93)	0.013 (0.93)	7.39×10^{-4} (0.91)
Saturated NaCl solution	2.298 (0.91)	0.313 (0.85)	0.019 (0.89)

To calculate the activation energy using the reaction rate coefficients (k) for the transformation reaction, the empirical Arrhenius treatment was used:

$$\log k = -[E_a/(2.303R)(1/T)] + A \quad (3)$$

where T is temperature in Kelvin and R is the gas constant (8.3145 J/mol/K). The empirical constants for activation energy, E_a, and A, can be deduced from the slope and intercept in plots of k as a function of temperature (1/T), as illustrated in Figure 5. When the activation energies (E_a) for the hydromagnesite to magnesite transformation in the two brines were determined, the following expression was used to calculate the rate coefficient (k_1) for a reaction at a specific temperature (T_1) from a known rate coefficient (k_2) determined at T_2:

$$\ln(k_1/k_2) = (E_a/R)(1/T_2 - 1/T_1) \quad (4)$$

The values of activation energies in the two brines and the estimated rate coefficients at 25°C are listed in Table 4. Based on the rate coefficients, the "half-life" times of the hydromagnesite (that is, the time required to transform one-half of the hydromagnesite into magnesite) at 25°C for GW brine and saturated NaCl solution are 73 years and 4.7 years, respectively.

Table 4. Calculated activation energies and the estimated rate coefficient at 25°C.

Brines	E_a (kJ/mol)	R^2	k ($hour^{-1}$)	Standard deviation
GW Brine	100	0.9984	1.085×10^{-6}	6.656×10^{-7}
Saturated NaCl solution	81	0.9831	1.699×10^{-5}	5.727×10^{-6}

It is important to note that the rate coefficients calculated herein are based on the rates representing the rapid portion of the transformation. As one can see in Table 2, transformation consists of two stages. In the first stage, the reaction progresses slowly, requiring nearly one-half of the total reaction time for only a few percent of hydromagnesite to convert to magnesite.

The induction period, in which about 4-5% of hydromagnesite was transformed into magnesite, may result from slow magnesite nucleation. Once nuclei of magnesite form, transformation accelerates. The duration of the induction period at 25°C was estimated using the Arrhenius equation and the high temperature data summarized in Table 2. The calculated rate coefficients

for transformation in saturated NaCl solution and GW brine at 25°C are 6.67×10^{-7} and 6.51×10^{-8} $hour^{-1}$, respectively. In other words, it would require about 18 and 200 years to initiate rapid transformation in the NaCl and GW brines, respectively. The relatively large standard deviations for the rate coefficients (about one order-of-magnitude) are attributed to the relatively large minimum quantifiable limit of XRD for magnesite at the onset of the transformation.

We attempted to estimate transformation half-life times using our data in Table 2 along with the rate equation in Sayles and Fyfe (1973), a fourth-order relationship between reaction time (t^4) and magnesite formation. Using that approach, half-life times were on the order of 3×10^7 and 4×10^4 years, for reactions in GW brine and NaCl solution, respectively. Those transformation times are significantly longer than those estimated for or observed in natural environments at Lake Bonneville (Graf et al., 1961) and in southeastern Australia (Alderman, 1965; von der Borch, 1965). It is likely that the fourth-order relationship used by Sayles and Fyfe (1973) is not applicable to our experimental system, which involves a more complex chemical system, and much higher ionic strengths.

Transformation Mechanisms

To elucidate transformation mechanisms, a series of experiments were conducted in which ionic strengths, magnesium concentrations, and sulfate concentrations were varied. Two hypotheses for reaction mechanisms were considered. We considered the direct dehydration of hydromagnesite in which water molecules in the hydromagnesite structure are liberated and the mineral restructures to form magnesite and brucite:

$$4MgCO_3 \bullet Mg(OH)_2 \bullet 4H_2O \leftrightarrow 4MgCO_3 + Mg(OH)_2 + 4H_2O \quad (5)$$

We also considered precipitation of magnesite from Mg^{2+} and CO_3^{2-} that are liberated through dissolution of hydromagnesite.

The two hypothesized reaction mechanisms may occur simultaneously during the reaction, but it is likely that one will dominate in at least some cases. If the dissolution/precipitation dominates

transformation, the concentration of Mg in the solution would affect hydromagnesite dissolution rate and, therefore, decrease the formation rate of magnesite. To test this, reaction rate measurements were made in solutions with different concentrations of Mg and SO_4. Alternatively, if the conversion process is dominated by dehydration of hydromagnesite, the effect of Mg concentration may be small, or even negligible. Water activity, however, may affect dehydration of hydromagnesite, and was also tested by measuring extents of transformation in NaCl solutions of varying ionic strengths. The results of these various tests are summarized in Table 5. All of these experiments were conducted at 200°C for 2 hours, a combination allowing uniformity for comparison yet providing conditions where partial transformation was observed in most cases.

Table 5. Extent of hydromagnesite to magnesite transformation as a function of solution composition (temperature = 200°C; reaction time = 2.0 hours).

(Matrix 1)		(Matrix 2)		(Matrix 3)		(Matrix 4)		
As function of NaCl ionic strength		As function of [Mg] in GW brine		As function of $[MgCl_2]$ in saturated NaCl solution		As function of $[MgSO_4]$ in saturated NaCl solution		
DF*	wt% magnesite	[Mg] g/L	wt% magnesite	[Mg] g/L	wt% magnesite	[Mg] g/L	$[SO_4]$ g/L	wt% magnesite
1/20	2.0	0.00	100	0.26	100	0.00	0.00	96
1/10	2.3	1.24	49	0.51	100	1.00	4.06	42
1/5	3.8	2.47	5.3	2.57	100	2.50	10.15	5.0
3/5	21	4.95	2.2	5.15	51	5.00	20.31	2.5
4/5	87	12.37	1.6	10.30	10	7.50	33.85	1.6
				12.37	4.7			

*DF = dilution factor of saturated NaCl solution (5.6M) expressed in volume fraction. For example, a DF of 1/20 indicates 1 part saturated NaCl solution diluted to 20 parts solution.

The results in Table 5 indicate that three factors significantly influence the reaction rate. At NaCl concentrations less than or equal to 1/5 of its saturation concentration (that is, ≤1.1M), formation of magnesite is limited (during the 2-hour reaction period). Greater NaCl

concentrations result in significant extents of transformation. This observation supports the hypothesis that dehydration of hydromagnesite is important, in that higher NaCl concentration would promote the dehydration shown in equation (5).

In NaCl brine, transformation rate is also affected by magnesium concentration (Table 5, Matrix 3). Increased magnesium concentration (as $MgCl_2$) significantly decreases the transformation rate of hydromagnesite to magnesite, at concentrations greater than or equal to 5.15 g/L Mg. This effect may stem from magnesium inhibiting dissolution of hydromagnesite.

The effect of magnesium concentration on transformation in GW brine is significantly different, in that much less magnesium is required to significantly diminish transformation rates (Table 5, compare Matrix 2 and Matrix 3 results). This may be due to the presence of 0.18M SO_4 in the GW brine (Table 1), which would impact the formation rate of magnesite through a complexation process:

$$Mg^{2+} + SO_4^{2-} \leftrightarrow MgSO_{4(aq)} \qquad (6)$$

The aqueous complex of magnesium sulfate reduces the activity of Mg^{2+} in the solution and, consequently, reduces the formation rate of magnesite (R_{MgCO3}) from dissolved magnesium and carbonate:

$$R_{MgCO3} = k_p(Mg^{2+})(CO_3^{2-}) \qquad (7)$$

where k_p is the precipitation rate coefficient. This hypothesis is indirectly verified by the results of experiments conducted in mixtures of $MgSO_4$ in NaCl solutions (Table 5, Matrix 4). At similar magnesium concentrations, transformation rates in GW brine and NaCl solution amended with $MgSO_4$ (Table 5, Matrix 2 and Matrix 4, respectively) are also similar. In both cases, the sulfate ligand is available to reduce activity of Mg^{2+}. It is not likely that in saturated NaCl solutions, the formation of $MgCl^+$ would be responsible for a significant decrease in Mg^{2+} activity, because that species is a weakly associated complex (log K_{MgCl^+} = -0.1349; Wolery, 1992). In contrast, magnesite precipitation rate would be decreased significantly by the presence

of SO_4 through formation of $MgSO_4$, because it is a strongly associated aqueous complex (log $K_{MgSO4(aq)} = 2.4117$; Wolery, 1992). In summary, the dominant transformation mechanism in GW brine is dissolution - precipitation. The presence of sulfate in GW brine promotes the dissolution of hydromagnesite, but formation of $MgSO_4$ complexes reduces magnesite precipitation rate.

Inferences from TEM Examinations

Additional information on reaction mechanisms was obtained with TEM examination of reaction products from experiments conducted in saturated NaCl solution and in GW brine. Figures 6 and 7 show the morphologies of minerals as well as the electron diffractions of products in the saturated NaCl and GW brines, respectively. Figure 6a, in which only 5% of added hydromagnesite was transformed into magnesite, shows the coexistance of the reactant, hydromagnesite, and product, magnesite in the reaction system. The rapid dehydration processs resulted in pyramidal-shaped precipitates, Figure 6b. The original accicular morphology of hydrmagnesite becomes blurred and indistincted because of dehydration. This observation appears similar to that described by Spötl and Burns (1994), in which hydromagnesite shrinking preceeds formation of magnesite. When about 95% of hydroxymagnesite was transformed into magnesite, the pyramidal-shaped precipitates are the dominant product, Figure 6b, and are identified as magnesite by XRD.

In contrast, the magnesite formed in GW brine occurs as highly uniform rhombohedra (Figure 7b). This morphology has been observed by others in natural settings, as well as in laboratory experiments configured so that magnesite was slowly crystallized from solution in the presence of magnesium (Sayles and Fyfe, 1973). The acicular nature of the hydromagnesite is still discernable (Figure 7a), indicating less dehydration compared to that in the saturated NaCl solution (Figure 6a). The differences in morphologies of hydromagnesite in these two brines supports conclusions drawn from the aqueous chemistry experiments, in that magnesite is formed by different pathways in the two brines. A dissolution-precipitation transformation process is dominant in GW brine due to a substantial magnesium concentration, whereas in the saturated NaCl brine, a dehydration transformation process is dominant. From XRD analysis,

both the minerals in Figure 6b and 7b are the crystallized magnesites, the electron diffraction pattern. The insert shows a sharp diffraction pattern for the product slowly formed in the GW brine, figure 7b. However, a diffuse diffraction pattern, Figure 6b, was obtained for the magnesite that formed rapidly in the pure NaCl brine. The diffuse nature of this pattern indicates a low-angle boundary in the crystals, or a less perfect structure as compared with that in Figure 7b.

Conclusions

Experiments, conducted at elevated temperatures to elucidate transformation mechanisms of hydromagnesite to magnesite, showed increased transformation rates with increased ionic strength and decreased magnesium concentrations. Sulfate concentration indirectly affected rates, and may act by reducing magnesium activity through complexation.

An "induction" period, an interval of minimal transformation, was observed at the beginning of all experiments. At 25°C, the induction period is estimated to require 18 to 200 years, with the longer times attributed to higher magnesium concentrations. Once the induction period is completed, and more rapid transformation begins, the corresponding "half-lives" of hydromagnesite are about 4.7 and 73 years. Activation energies for the rapid transformation period were estimated to be between 81 and 100 kJ/mol.

Two mechanisms for the transformation are supported. In brines with low magnesium concentration, hydromagnesite dehydration with concomitant formation of brucite and magnesite is favored. In brines with high magnesium concentration, a hydromagnesite dissolution – magnesite precipitation process is favored. Those mechanisms are also supported by TEM observations of reaction products.

Acknowledgements

Sandia National Laboratories is a multi-program laboratory operated by Sandia Corporation, a Lockheed-Martin Company, for the United States Department of Energy under Contract DE-

ACO4-94AL85000. The work conducted for WIPP described in this paper was conducted under the Sandia NWMP Quality Assurance Program which is equivalent to NQA-1, NQA-2 (Part 2.7), and NQA-3 Standards. The authors thank Dr. Huifang Xu, University of New Mexico, for his help with TEM analyses. We also thank Dr. Yifeng Wang, Sandia National Laboratories, for his helpful review of this paper.

Literature Cited

Alderman, A.R., 1965. Dolomitic Sediments and Their Environment in the South-East of South Australia. Geochimica et Cosmochimica Acta. Vol. 29, 1355-1365.

Brady, P.V., J.L. Krumhansl, and H.W. Papenguth, 1996. Surface Complexation Clues to Dolomite Growth, Geochimica et Cosmochimica Acta. Vol. 60, 727-731.

Bynum, R.V., C.T. Stockman, H.W. Papenguth, Y. Wang, A.C. Peterson, J.L. Krumhansl, E.J. Nowak, J. Cotton, S.J. Patchet, and M.S.Y. Chu, 1999. "Identification and Evaluation of Appropriate Backfills for the Waste Isolation Pilot Plan (WIPP)," in D.G. Bennett, H.W. Papenguth, M.S.Y. Chu, D.A. Galson, S.L. Duerden, and M.L. Matthews (editors), International Workshop on the Uses of Backfill in Nuclear Waste Repositories, Carlsbad, New Mexico, US, May 1998. Bristol, United Kingdom, Environment Agency, R&D Technical Report P178, p. 2-178 to 2-187.

Davies, P.J., B. Bubela, 1973. The Transformation of Nesquehonite into Hydromagnesite, Chemical Geology, Vol. 12, 289-300.

Graf, D.L., A.J. Eardley, N.F. Shimp, 1961. A Preliminary Report on Magnesium Carbonate Formation in Glacial Lake Bonneville, The Journal of Geology, Vol. 69, 219-223.

Krumhansl, J.L., K.M. Kimball, C.L. Stein, 1991. Intergranular Fluid Compositions from the Waste Isolation Pilot Plant (WIPP), Southeastern New Mexico. SAND90-0584. Albuquerque, NM: Sandia National Laboratories.

Langmuir, D., 1965. Stability of Carbonates in the System $MgO-CO_2-H_2O$, J. of Geology. Vol. 73, 730-754.

Lippmann, F., 1973. Sedimentary Carbonate Minerals. New York, NY: Springer-Verlag. 71-87.

Papenguth, H.W., J.L Krumhansl, R.V. Bynum, Y. Wang, J.W. Kelly, H.L. Anderson, E.J. Nowak, 1999. "Status of Research on Magnesium Oxide Backfill," in D.G. Bennett, H.W. Papenguth, M.S.Y. Chu, D.A. Galson, S.L. Duerden, and M.L. Matthews (editors), International Workshop on the Uses of Backfill in Nuclear Waste Repositories, Carlsbad, New Mexico, US, May 1998. Bristol, United Kingdom, Environment Agency, R&D Technical Report P178, p. 3-43 to 3-63.

Sayles, F.L., W.S. Fyfe, 1973. The Crystallization of Magnesite from Aqueous Solution, Geochimica et Cosmochimica Acta. Vol. 37, 87-99.

Spötl, C., S.J. Burns, 1994. Magnesite Diagenesis in Redbeds: A Case Study from the Permian of the Northern Calcareous Alps (Tyrol, Austria), Sedimentology. Vol. 41, 543-565.

Stamatakis, M.G., 1995. Occurrence and Genesis of Huntite-Hydromagnesite Assemblages, Kozani, Greece-Important New White Fillers and Extenders, Applied Earth Science. Vol. 104, B179-B210.

US DOE (Department of Energy). 1996. Title 40 CFR Part 191 Compliance Certification Application for the Waste Isolation Pilot Plant. DOE/CAO-1996-2184. Carlsbad, NM: United States Department of Energy, Waste Isolation Pilot Plant, Carlsbad Area Office.

von der Borch, C., 1965. The Distribution and Preliminary Geochemistry of Modern Carbonate Sediments of the Coorong Area, South Australia, Geochimica et Cosmochimica Acta. Vol. 29, 781-799.

Wolery, T.J., 1992. EQ3NR, A Computer Program for Geochemical Aqueous Speciation-Solubility Calculations: Theoretical Manual, User's Guide, and Related Documentation (Version 7.0). UCRL-MA-110662-PT. 3. Livermore, CA: Lawrence Livermore National Laboratory. (Available from the National Technical Information Service, Springfield, VA, 22161, Telephone: 703/487-4650 as DE93005827/XAB.)

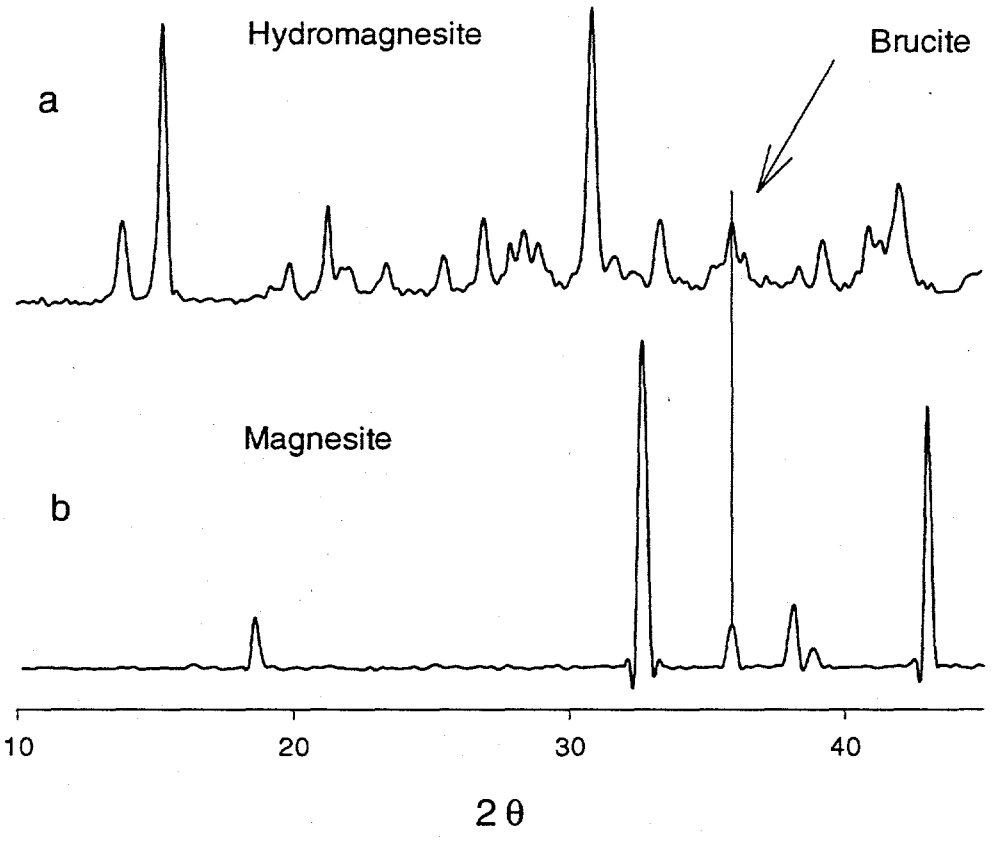

Figure 1. X-ray diffraction pattens for hydromagnesite (a) and magnesite (b) used in this study. Hydromagnesite used as reactant and standard and magnesite is used for establishing the calibration curve.

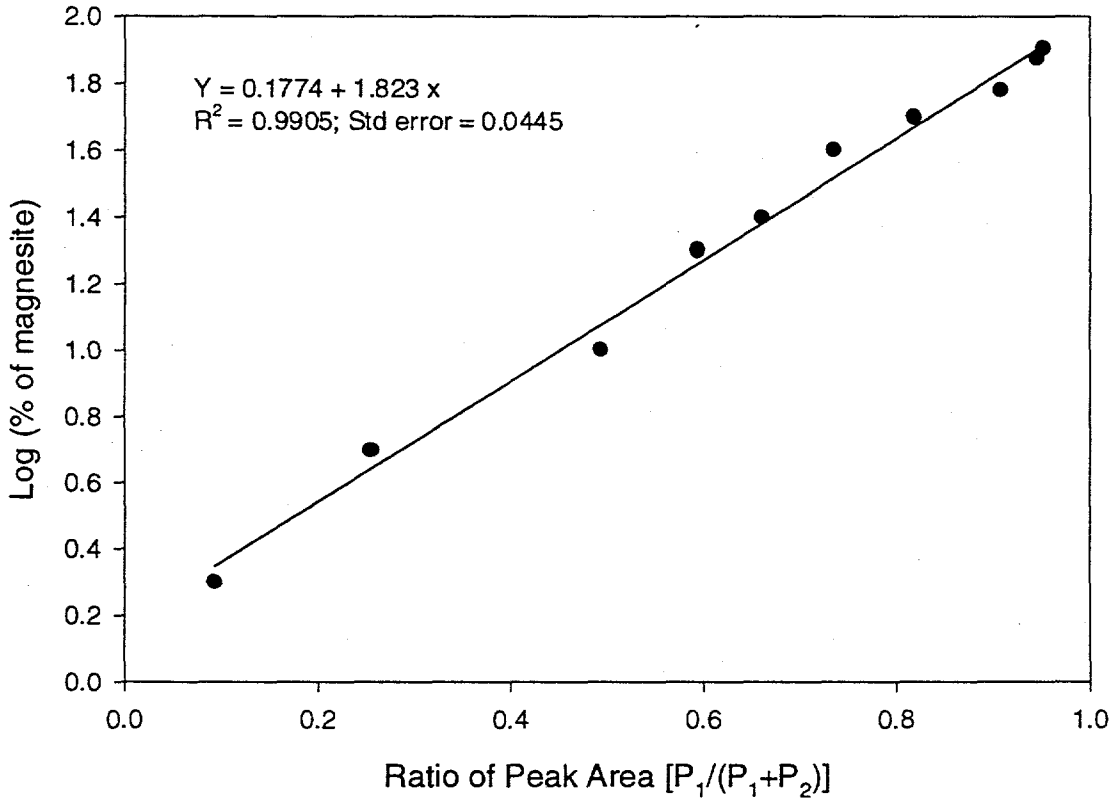

Figure 2. Calibration curve for determining magnesite formed in the reacted solids from hydromagnesite incubated with brine.

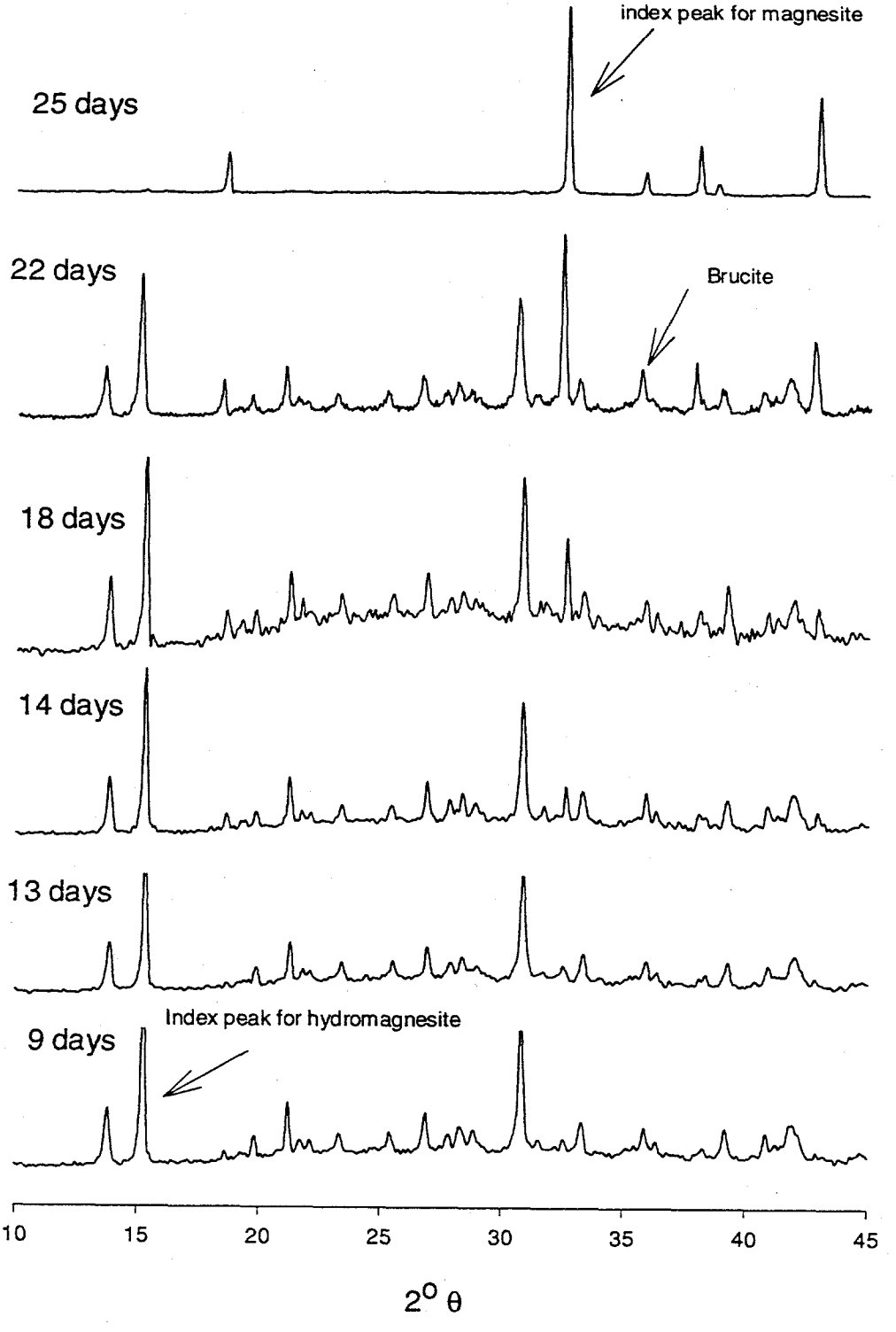

Figure 3. Transformation of hydromagnesite to magnesite as a function of reaction time in saturated NaCl solution at 110°C.

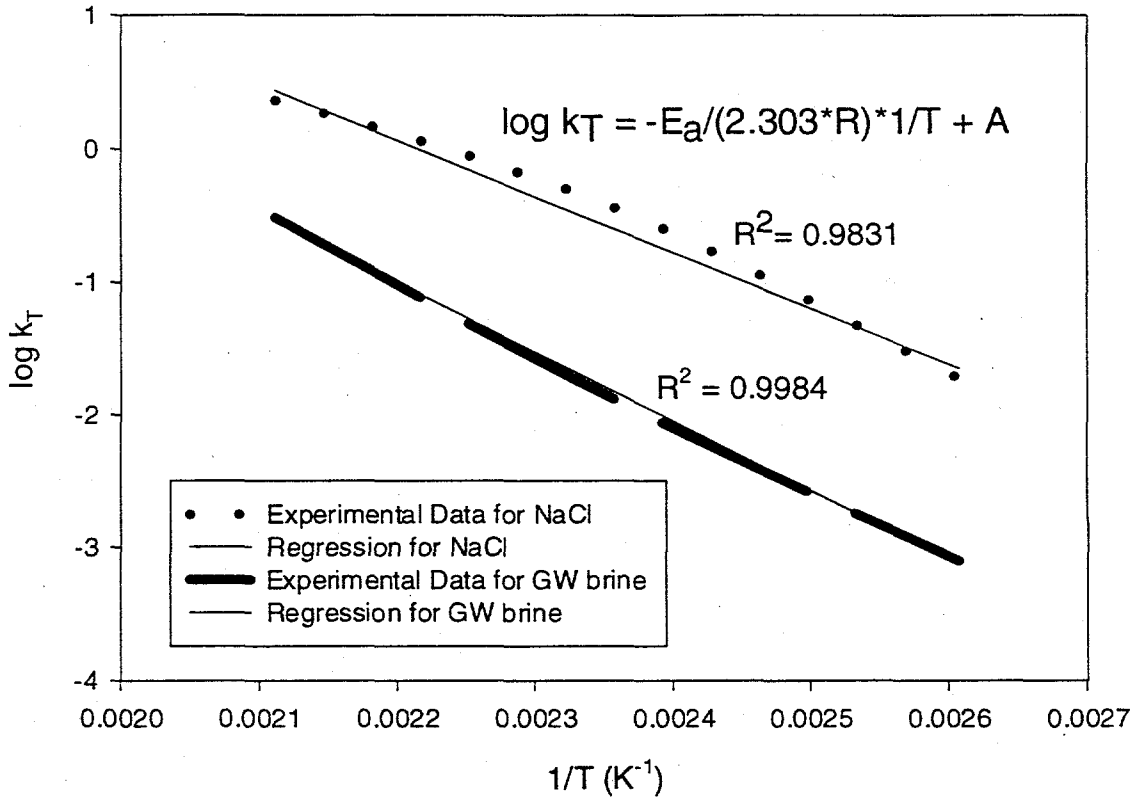

Figure 5. Calculation of activation energies (Ea) for both brines

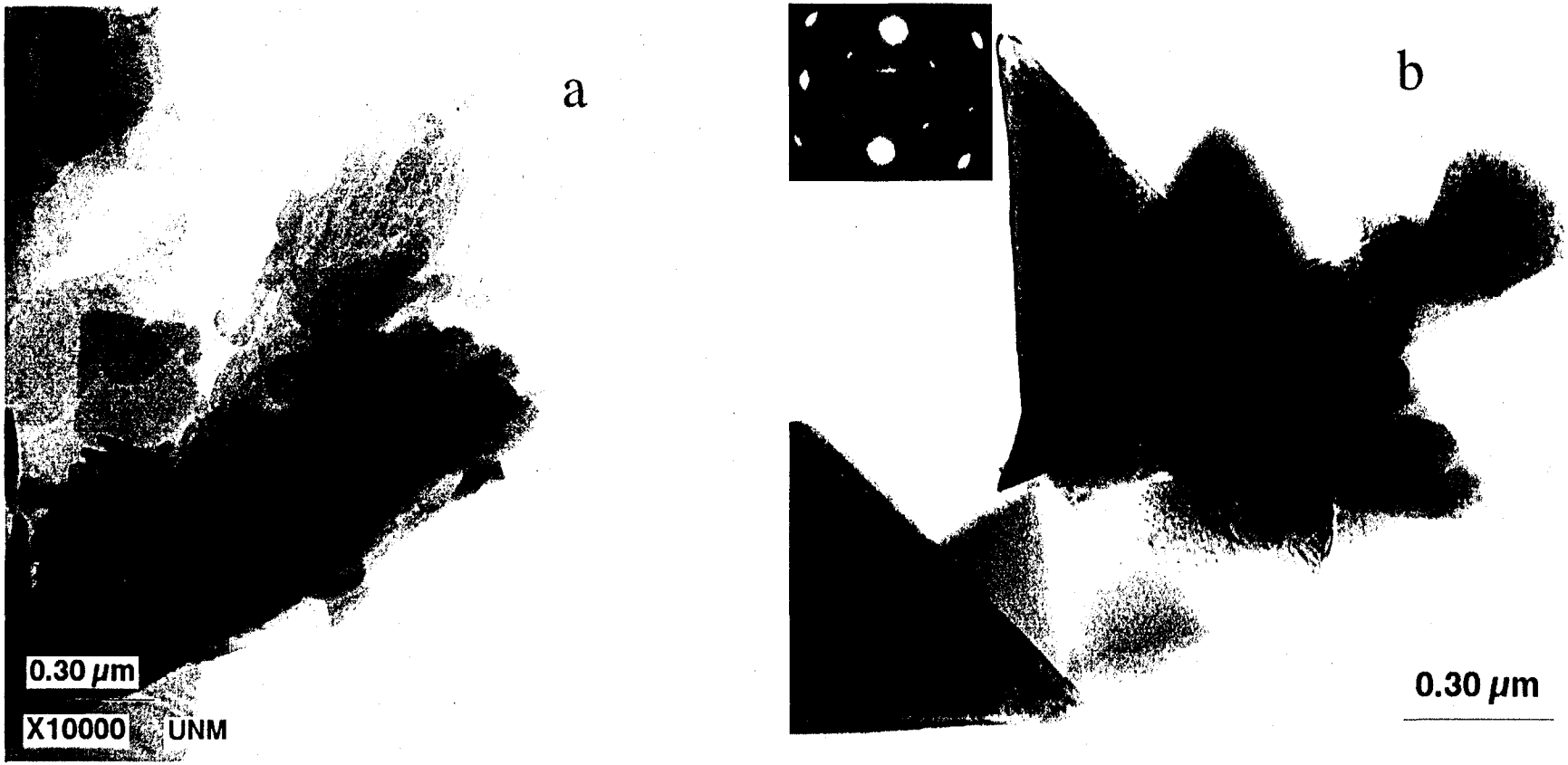

Figure 6. TEM images for solids collected in saturated NaCl solutions when approximately 5% (a) and 95% (b) of hydromagnesite were transformed into magnesite at 200°C, respectively. The insert in (b) is the electronic diffraction pattern, indicating a low-angle boundary for the magnesite crystals that formed rapidly in the NaCl solution.

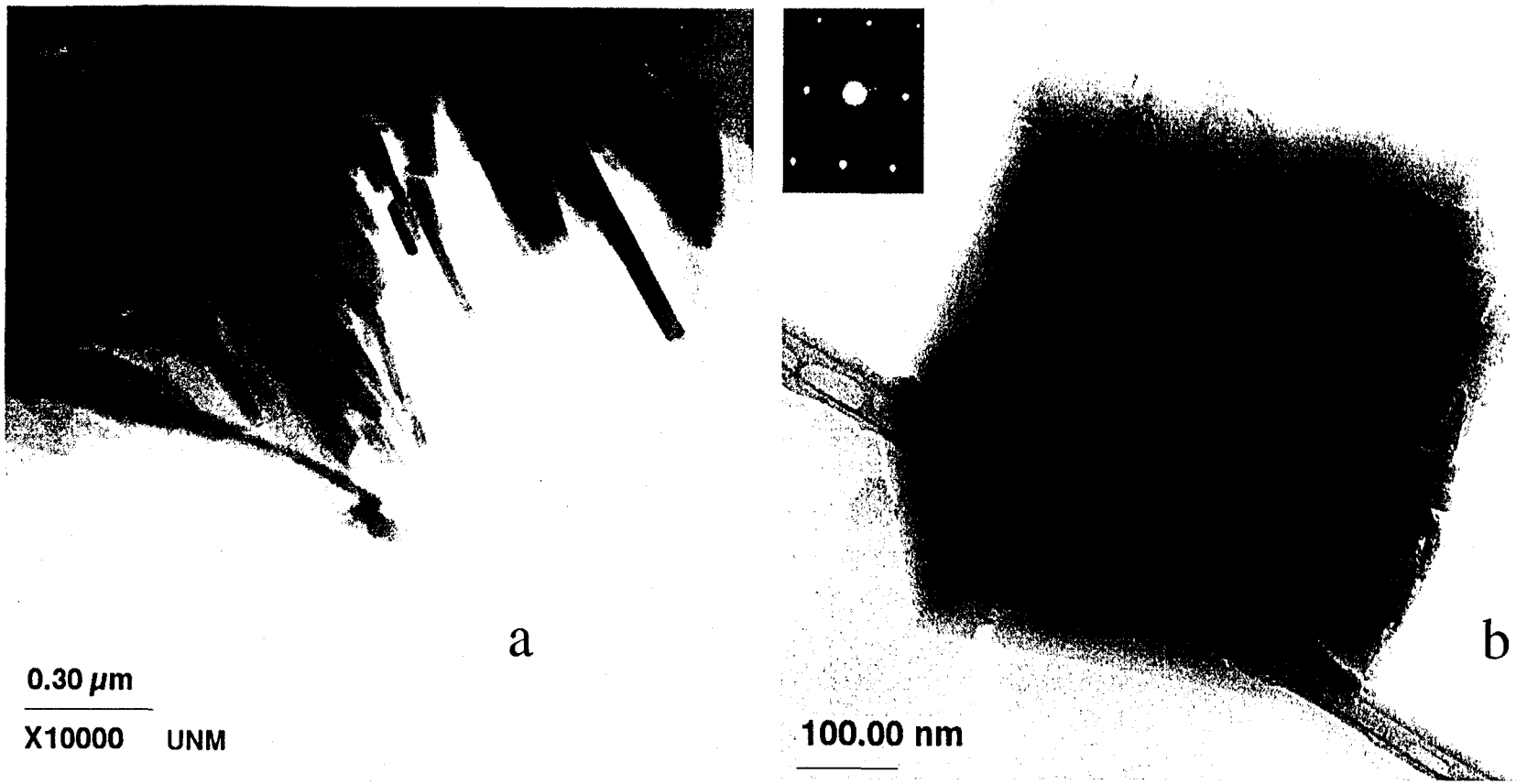

Figure 7. TEM images for solids collected in GW brine when approximately 5% (a) and 95% (b) of hydromagnesite were transformed into magnesite, respectively, at 200°C. The insert in (b) is the electronic diffraction pattern for the magnesite slowly formed in the GW brine. The sharp characteristic of the diffraction pattern indicates a highly crystalline structure.